# The adsorption capacity of the base layer of pervious concrete pavement prepared with additives for typical runoff pollutants

**Wang Junling[1], Wei Jiangtao[1,*], Wang Xueming[2], Feng Cuimin[1], Chen Tao[1], Sun Lihua[1] and Li Junqi[1]**

[1]Key Laboratory of Urban Stormwater System and Water Environment, Ministry of Education, Beijing University of Civil Engineering and Architecture, Beijing 100044, China
[2]Beijing Yanqing Municipal Commission of Urban Planning, Beijing 102100, China

**Additives were added to pervious concrete pavement to improve the removal capacity for runoff contaminants. In this study, static isothermal adsorption experiments were conducted for concrete prepared with fly ash or bentonite. The results showed that the material containing bentonite showed better adsorption capacity for runoff contaminants. The saturated adsorption values of bentonite for major runoff pollutants, including chemical oxygen demand (COD), total phosphorus (TP) and copper (Cu) were 8.61, 6.93, 19.31 mg/g respectively. However, the two additives showed only weak adsorption capacity for total nitrogen (TN). Compared to hardened cement, the adsorption capacity for COD, TP and Cu of the cement with bentonite was increased by 54%, 30% and 42% respectively, and the capacity of cement with fly ash increased by 42%, 11% and 33% respectively. Therefore, additives can improve the decontamination capacity of the base layer of the pervious concrete pavement. This study provides technical support for the construction of a sponge city.**

**Keywords:** Adsorption, base layer, optimization, pervious concrete pavement.

CHINA is vigorously promoting the construction of a sponge city to ease urban waterlog, prevent water pollution and beautify the environment. A sponge city is an urban environment that is planned and constructed to act as a sponge to soak up rain water for reuse. Instead of devising strategies to move rainwater away, a sponge city retains the water for use within the city. A pervious concrete pavement can serve as part of a sustainable drainage system to allow the collection, storage, purification and recharging of underground water. The construction of the pervious concrete pavement is generally designed to consist of four parts, i.e. the cushion, the sub-base, the base layer and the surface layer[1]. Studies have shown that the effect of the pervious concrete pavement on removal of stormwater runoff mainly depended on the surface layer. The base layer (including the sub-base) accounted for 2/3 of the volume of the pervious concrete pavement, but the contribution to the removal rate for runoff pollutants was only 10–25%, out of proportion to the thickness. Recent efforts to strengthen or modify the base layer of the pervious concrete pavement mainly considered the effects of aggregate type and porosity on drainage performance[2–5]. However, there have been few studies on the ability to modify concrete by using additives to improve runoff pollutant removal of the base layer. To improve the removal of runoff contaminants and the deficiency of the base layer of the pervious concrete pavement, this study focused on strengthening the base layer of the pervious concrete pavement through the use of additives.

The additives must have strong adsorption capacity for runoff pollutants and be economically priced to allow widespread application. Here, fly ash and bentonite were used as additives to strengthen the function of the base layer.

Fly ash exhibits a loose and porous structure with small particles, a large specific surface and many active sites of Al and Si. Fly ash in cement allows the removal of runoff pollutants by surface charge adsorption and ion binding[2,3]. Fly ash is an abundant industrial waste with the world production estimated at over 750 million tonnes/year (refs 6, 7). Thus, it is economical and environmentally friendly to use fly ash as a cement additive.

Bentonite is also used as an additive for pervious concrete to improve the removal efficiency of runoff pollutants. In China, the bentonite reserve is 24,600 billion tonnes, 60% of the world reserve[6]. The molecular structure of bentonite is composed of two layers of Si–O tetrahedron that sandwich a layer of octahedral Al–O. $Si^{4+}$ can be replaced by $Al^{3+}$ or $Fe^{3+}$ in the tetrahedron and $Al^{3+}$ can be replaced by $Mg^{2+}$ or $Fe^{3+}$ in the octahedral, so the bentonite lattice can absorb the external cationic charge by means of static electrical charge effect to remove runoff pollutants[5,8].

There are many potential pollutants in storm water runoff. Dissolved total nitrogen (DTN) constitutes the majority of total nitrogen in storm water runoff[9]. DTN includes dissolved organic nitrogen and inorganic nitrogen. The inorganic nitrogen accounts for 60–70% of DTN and mainly exists as $NO_x$ and $NH_4^+$ in runoff[10,11]. Phosphate is the main phosphorous component[12] and was reported to constitute 70.9% of total phosphorus[13]. Additionally, chemical oxygen demand (COD) and copper (Cu) levels make runoff unsafe and the reduction of these parameters is a goal of a sponge city.

The results showed that the material containing bentonite showed better adsorption capacity for runoff contaminants. The saturated adsorption values of bentonite for major runoff pollutants, including COD, total phosphorus (TP) and Cu were 8.61, 6.93, 19.31 mg/g respectively. The saturated adsorption values of fly ash for major runoff pollutants, including COD, TP

*For correspondence. (e-mail: 328461564@qq.com)

**Table 1.** Composition of ordinary Portland cement

| Components | CaO | $SiO_2$ | $Al_2O_3$ | MgO | $K_2O$ | $Na_2O$ | $Fe_2O_3$ | $SO_3$ |
|---|---|---|---|---|---|---|---|---|
| Content (%) | 61.0 | 21.0 | 5.4 | 4.6 | 3.7 | 2.9 | 1.2 | 0.2 |

**Table 2.** The physical and chemical properties of ordinary Portland cement

| Specific surface area ($m^2$/kg) | Initial setting time (min) | Final setting time (min) | 3 days compressive strength (MPa) | 28 days compressive strength (MP) | 3 days flexural strength (MPa) | 28 days flexural strength (MPa) |
|---|---|---|---|---|---|---|
| ≥350.0 | ≥45.0 | ≤390.0 | ≥22.0 | ≥42.5 | ≥4.0 | ≥6.5 |


**Figure 1.** Materials. ***a***, Ordinary portland cement; ***b***, bentonite; ***c***, fly ash.

and Cu were 7.97, 6.24, 16.17 mg/g respectively. However, the two additives showed only weak adsorption capacity for total nitrogen (TN). Compared to hardened cement, the adsorption capacity for COD, TP and Cu of the cement with bentonite was increased by 54%, 30% and 42% respectively, and the capacity of cement with fly ash was increased by 42%, 11% and 33% respectively.

This study used three adsorption isotherms to show the adsorption capacity of additives to runoff pollutants and provides the theoretical foundation for improving the pollutant removal and the purification capability of the pervious concrete pavement. The study provides guidance for wide application of the pervious concrete pavement in the construction of a sponge city.

Ordinary Portland cement PO42.5 was used; the main components and the physical and chemical properties are shown in Figure 1 and Tables 1 and 2 respectively.

Fly ash and bentonite were used at 20% of cement weight. The ordinary Portland cement and two additives are shown in Figure 1, and the main components of bentonite and fly ash are shown in Tables 3 and 4 respectively.

The chemical reagents utilized in this study, including $C_6H_{12}O_6{\cdot}H_2O$, $KH_2PO_4$, $NH_4Cl$, $CuCl_2{\cdot}2H_2O$, $ZnCl_2$ and $PbCl_2$, are of analytical grade and were obtained from Hach Compamy, US.

A thermostatic shaking gas bath (Shanghai Bingyue Electronic Instrument Co Ltd), a digestion instrument (DRB200 Hach Company, US), and a portable visible spectrophotometer (DR1900 Hach Company US, with a measuring accuracy of 0.01 mg/l; Figure 2) were used in this experiment. The thermostatic shaking gas bath ensured that the reaction proceeded at constant temperature. The digestion instrument and portable visible spectrophotometer were used to measure the solution concentration of pollutants.

To evaluate the prepared materials, the adsorption isotherms were measured. Cement without additive was compared to cement with 20% fly ash or bentonite. The prepared materials were used as hardened cement blocks. The hardened cement blocks were grounded to powder and made into three adsorbents.

Four experiments were set up to measure the adsorption capacity of COD, TN, TP and Cu respectively. In each experiment 7 groups were set up. In a group, three adsorbents (5 g) were placed separately in three erlenmeyer flasks. The contaminant solutions were prepared in a volume of 100 ml at a solid-to-liquid ratio of 1 : 20 as shown in Figure 3.

Each contaminant solution was diluted to seven different concentrations as shown in Table 5. Every kind of adsorbent (5 g) was mixed with 4 kinds of contaminant solution respectively. Each contaminant solution was 100 ml and the concentrations of contaminant are shown in Table 5.

Each set of conical vials was placed in the thermostatic shaking gas bath and oscillated for 24 h at 25°C and 150 r/min. The digestion instrument and portable visible spectrophotometer were used to measure the residual concentration of adsorbates before and after filtration.

The data were fitted to three isothermal adsorption models that are widely used in adsorption modelling, the Langmuir model, the Freundlich model and the Temkin model[14–16].

Langmuir adsorption model

$$q_e = \frac{b \times q_m \times C_e}{1 + C_e}, \quad (1)$$

where $q_e$ is the equilibrium adsorption capacity (mg/g), $q_m$ is the theoretical saturated adsorption capacity of unit mass adsorbent, mg/g, $C_e$ is the adsorbate equilibrium concentration, mg/l, and $b$ is the Langmuir equilibrium

adsorption constant that can reflect the adsorption capacity of the additive.

The Langmuir adsorption model is an ideal model in which the adsorption heat does not change during adsorption and which represents the adsorption of a monomolecular layer. The Langmuir model assumes monomolecular adsorption, a uniform additive surface, and no interaction between the two molecules.

The theoretical saturated capacity of unit mass $q_m$ is a quantity index, but the values of $q_m$ with different working conditions show significant discrepancy. Therefore, it is difficult to predict the adsorption capacity of additives with $q_m$ (refs 17, 18). The Langmuir adsorption equilibrium constant $b$ can reflect the adsorption affinity of additives. The smaller the $b$ value, the stronger the adsorption affinity[19].

Freundlich adsorption model

$$q_e = K_F \times C_e^{1/n}, \quad (2)$$

where $q_e$ is the equilibrium adsorption capacity (mg/g), $C_e$ is the equilibrium concentration of adsorbate (mg/l); $F_K$ is the characteristic parameter that reflects the adsorption capacity, and $n$ is the adsorption index that represents the intrinsic property of the additive.

The Freundlich adsorption model is an isothermal adsorption equation based on experience. During adsorption, heat decreases logarithmically as the adsorption capacity decreases, consistent with bimolecular layer adsorption on a non-uniform surface. The Freundlich adsorption model describes a non-uniform surface with multi-molecular layer adsorption based on the heterogenous surface[20,21]. $K_F$ and $n$ are Freundlich constants that represent the adsorption capacity and intensity respectively. $K_F$ is a constant related to the maximum adsorption capacity. $N$ defines extent of linearity of the adsorption which can reflect the affinity between the additive and the adsorbate. Adsorption occurs easily at $b = 2–10$, but the adsorption is more difficult when $n$ is less than 0.5 (refs 14, 22).

Temkin adsorption model

$$q_e = A + B \times \ln C_e, \quad (3)$$

where $q_e$ is the equilibrium adsorption capacity, mg/g, $C_e$ is the equilibrium concentration of adsorbate, mg/l, and A and B are constants. The Temkin adsorption model is an isothermal adsorption model based on the fact that the heat of adsorption of all molecules in the layer decreases linearly and it takes adsorbate–adsorbent interactions into account[23].

We tested typical runoff pollutants of COD, TN, TP and Cu using glucose, $NH_4Cl$, $KH_2PO_4$ and $CuCl_2{\cdot}2H_2O$ respectively.

The simulation results of COD adsorption process of the hardened cement, the hardened cement with fly ash and the hardened cement with bentonite are shown in Figure 4. The fitting values of the parameters of the isothermal adsorption models are shown in Table 6.

Comparison of linear fitting coefficients between the three models shows that the Langmuir model and the Temkin model fit better than the Freundlich model, with fitting coefficients that are larger than 0.8. The results show that the Langmuir and Temkin models are more suitable for describing the adsorption of COD. Since the Temkin model is a chemisorption model, the additives likely remove COD via chemisorption.

The fitting parameter $b$ in the Langmuir model reflects the adsorption affinity of additives. The smaller the $b$ value, the stronger the adsorption affinity. The $b$ values were lowest for hardened cement with bentonite, followed by the hardened cement with fly ash, and finally untreated cement. Therefore, the order of adsorption capacity additives for COD from the highest to the lowest was hardened cement with bentonite, hardened cement with fly ash and untreated cement. The saturated adsorption of COD by the three additives are shown in Table 7.

The simulation results of TP adsorption are shown in Figure 5. The fitting values of the parameters of isothermal adsorption models is shown in Table 8.

According to the comparison of linear fitting models, the Langmuir and Freundlich models fit better than the Temkin model, with fitting coefficients greater than 0.8. Thus, the Langmuir and Freundlich models are more suitable for describing the adsorption process of TP.

**Table 3.** Composition of bentonite

| Components | Montmorillonite | Quartz | Feldspar |
|---|---|---|---|
| Content (%) | 86.0 | 12.0 | 2.0 |

**Table 4.** Composition of fly ash

| Components | $SiO_2$ | $Al_2O_3$ | $Fe_2O_3$ | CaO | MgO | $K_2O$ |
|---|---|---|---|---|---|---|
| Content (%) | 53.3 | 28.3 | 4.2 | 4.6 | 1.2 | 0.9 |


**Figure 2.** Experimental apparatus. ***a***, The thermostatic shaking gas bath; ***b***, the digestion instrument; ***c***, the visible spectrophotometer.

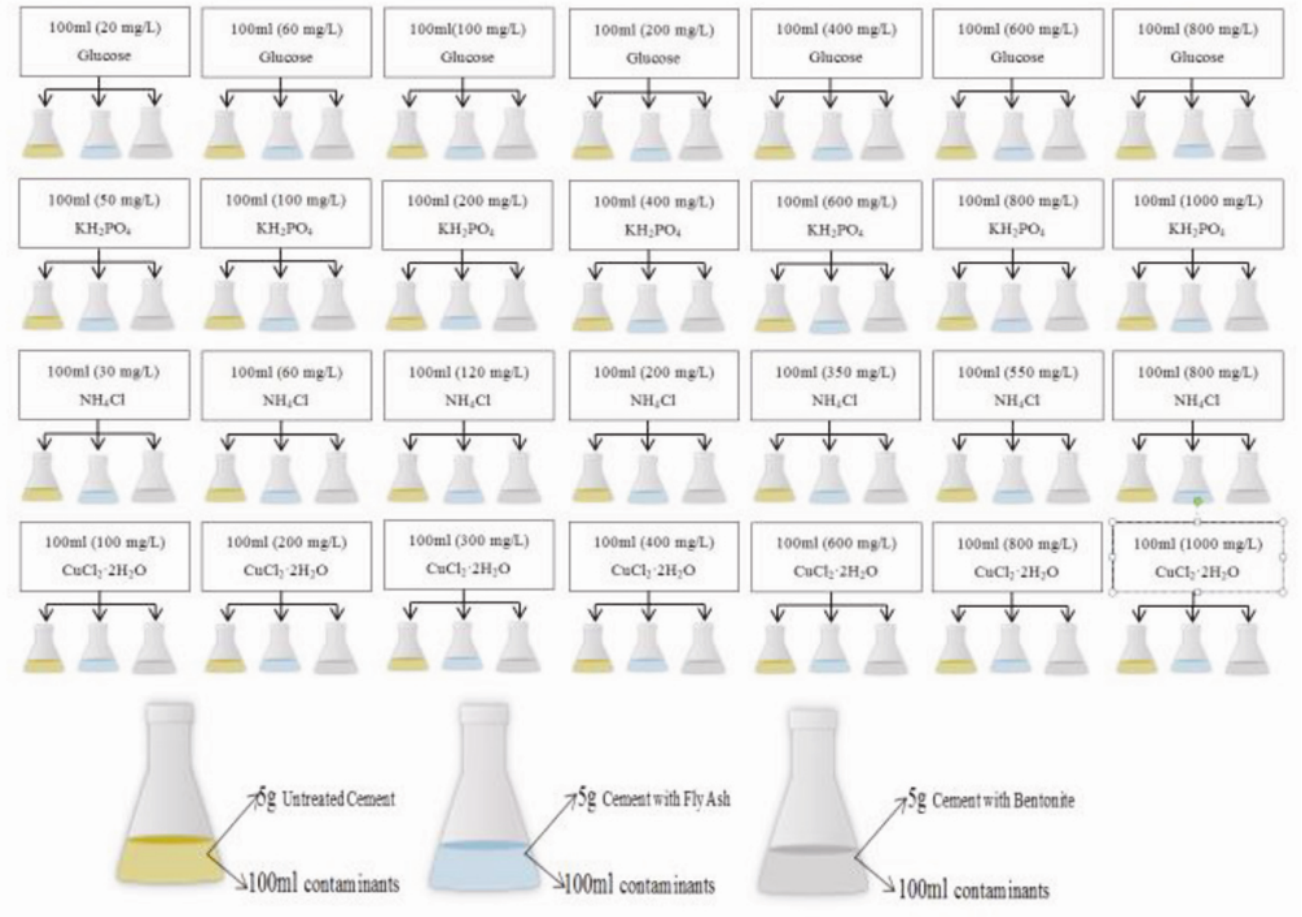


**Figure 3.** Experiment program.

**Table 5.** Tested concentrations of contaminants

| Experimental reagents | Concentration (mg/l) | | | | | | |
|---|---|---|---|---|---|---|---|
| Glucose | 20 | 60 | 100 | 200 | 400 | 600 | 800 |
| $KH_2PO_4$ (by the P) | 50 | 100 | 200 | 400 | 600 | 800 | 1000 |
| $NH_4Cl$ (by the N) | 30 | 60 | 120 | 200 | 350 | 550 | 800 |
| $CuCl_2{\cdot}2H_2O$ (by the Cu) | 100 | 200 | 300 | 400 | 600 | 800 | 1000 |

**Table 6.** Fitting values of parameters of isothermal adsorption models for COD

| | Langmuir model | | | Freundlich model | | | Temkin model | | |
|---|---|---|---|---|---|---|---|---|---|
| Additives | $q_m$ (mg/g) | $b$ (l/mg) | $R^2$ | $K_F$ | $n$ | $R^2$ | $A$ | $B$ | $R^2$ |
| Untreated cement | 6.79 | 0.0029 | 0.868 | 0.139 | 1.787 | 0.773 | –6.911 | 1.889 | 0.901 |
| Cement with fly ash | 7.97 | 0.0027 | 0.852 | 0.452 | 2.319 | 0.709 | –6.798 | 2.208 | 0.885 |
| Cement with bentonite | 8.61 | 0.0023 | 0.815 | 0.492 | 2.359 | 0.696 | –6.184 | 2.138 | 0.811 |

The $b$ value was lowest for hardened cement with bentonite, followed by the hardened cement with fly ash, and was the largest for untreated cement. Therefore, the adsorption capacity for TP was highest for hardened cement with bentonite, followed by cement with fly ash, and untreated cement was the lowest. The saturated adsorption value for TP exhibited by the three additives is shown in Table 9.

There was only very low removal of TN by the hardened cements (less than 8%); hence, the data were not fit to the models. The lack of TN removal is consistent with the study of Lei *et al.*[15], who reported a

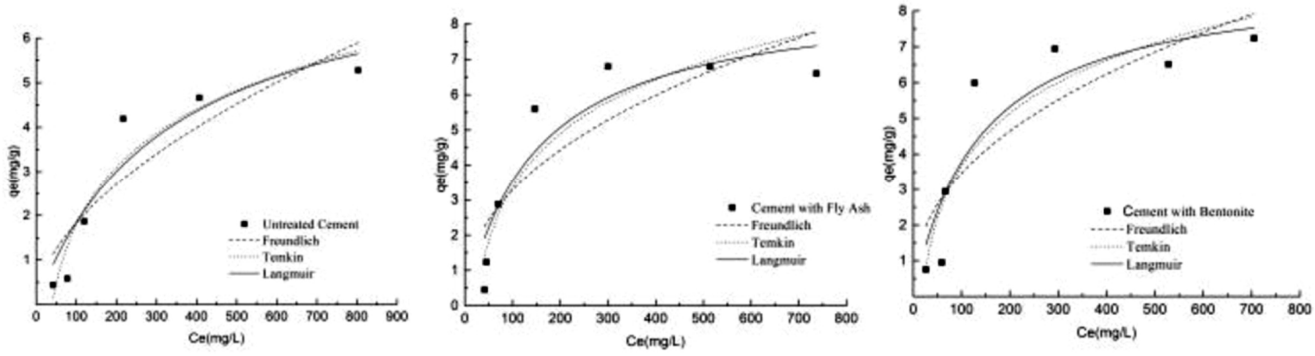


**Figure 4.** The simulation of COD adsorption.

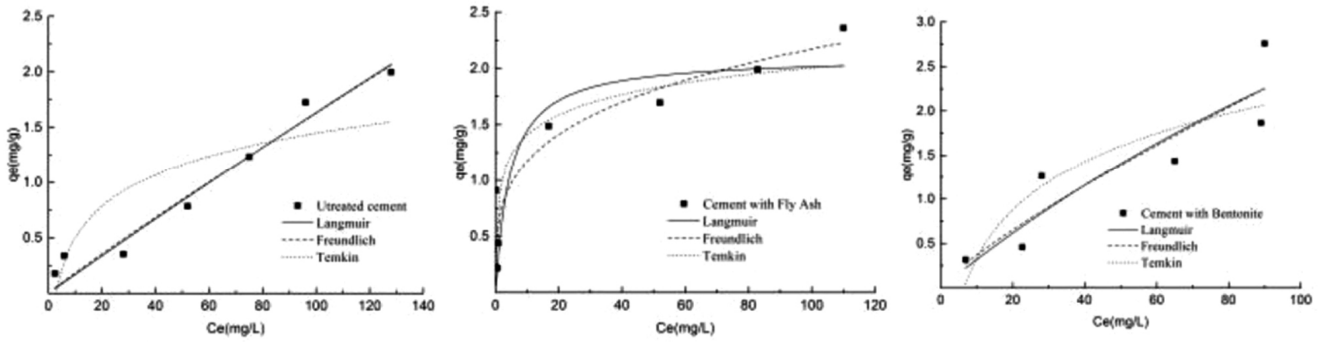


**Figure 5.** The simulation of TP adsorption.

**Table 7.** Saturated adsorption of COD

| Additives | Saturated adsorption capacity (mg/g) | Improvement compared with untreated cement |
|---|---|---|
| Untreated cement | 6.79 | – |
| Cement with fly ash | 7.97 | 17% |
| Cement with bentonite | 8.61 | 26% |

removal rate of 5.37% for TN by a porous hydrate biological filter with fly ash. In the study of Yu *et al.*[16], the removal rate of TN using a sequencing batch reactor (SBR) with bentonite was increased by 10.9%. Because the $NH_4Cl$ is acidic and adsorption capacity is influenced by pH, when the pH is greater than 5, the adsorption rate will be below 10% (ref. 24).

The simulation results of the Cu adsorption process are shown in Figure 6. The fitting values of parameters of isothermal adsorption models are shown in Table 10.

According to the comparison of linear fitting coefficients between the models, the Langmuir model fits better than the other two models, which had coefficients larger than 0.8. Thus, the Langmuir model is more suitable for describing the adsorption process for TP.

The *b* value was lowest for cement with bentonite, higher for cement with fly ash and highest for untreated cement. Therefore, the adsorption capacity for Cu is highest for cement with bentonite, followed by cement with fly ash, followed by untreated cement. The saturated adsorption value for Cu of the three additives is shown in Table 11.

The adsorption capacity improvement of the base layer of the pervious concrete pavement was limited. As the additives account for only 20% of the material, most runoff pollutants contact the cement. To improve pervious concrete pavement, future efforts should be made to increase the contact area between the additives and the runoff pollutants to enhance adsorption capacity.

The experimental results show that the removal capacity for runoff pollutants of the base layer of the pervious concrete pavement was improved by the use of additives. The isothermal adsorption model revealed that bentonite allows better removal capacity for runoff pollutants than fly ash. Compared to untreated cement, the adsorption capacities for the runoff pollutants (COD, TP and Cu) of the cement with bentonite increased by 26%, 38% and 39% respectively. The adsorption capacity of the hardened cement with fly ash increased by 17%, 24% and 16% respectively. However, both materials showed only

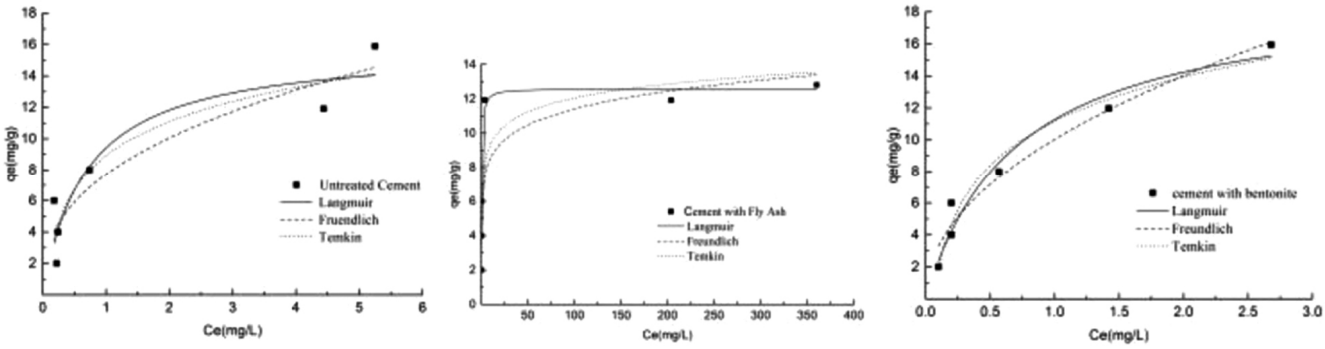


**Figure 6.** The simulation results of Cu adsorption.

**Table 8.** Fitting values of parameters of isothermal adsorption models for TP

| | Langmuir model | | | Freundlich model | | | Temkin model | | |
|---|---|---|---|---|---|---|---|---|---|
| Materials | $q_m$ (mg/g) | $b$ (l/mg) | $R^2$ | $K_F$ | $n$ | $R^2$ | $A$ | $B$ | $R^2$ |
| Cement | 5.01 | 0.008 | 0.851 | 0.091 | 1.576 | 0.888 | –0.369 | 0.424 | 0.781 |
| Cement with fly ash | 6.24 | 0.005 | 0.906 | 0.203 | 1.990 | 0.946 | 0.372 | 0.322 | 0.836 |
| Cement with bentonite | 6.93 | 0.002 | 0.913 | 0.047 | 1.126 | 0.915 | –1.747 | 0.892 | 0.791 |

**Table 9.** Saturated adsorption for TP

| Additives | Saturated adsorption capacity (mg/g) | Improvement compared with untreated cement |
|---|---|---|
| Untreated cement | 5.01 | – |
| Cement with fly ash | 6.24 | 24% |
| Cement with bentonite | 6.93 | 38% |

**Table 10.** Fitting values of parameters of isothermal adsorption models for Cu

| | Langmuir model | | | Freundlich model | | | Temkin model | | |
|---|---|---|---|---|---|---|---|---|---|
| Materials | $q_m$ (mg/g) | $b$ (l/mg) | $R^2$ | $K_F$ | $n$ | $R^2$ | $A$ | $B$ | $R^2$ |
| Cement | 13.88 | 1.529 | 0.835 | 7.702 | 2.611 | 0.854 | 8.910 | 3.140 | 0.842 |
| Cement with fly ash | 16.17 | 1.450 | 0.978 | 6.725 | 2.937 | 0.898 | 7.498 | 2.583 | 0.971 |
| Cement with bentonite | 19.31 | 1.40 | 0.954 | 10.02 | 2.070 | 0.962 | 11.16 | 4.011 | 0.962 |

**Table 11.** Saturated adsorption for Cu

| Additives | Saturated adsorption capacity (mg/g) | Improvement compared with untreated cement |
|---|---|---|
| Untreated cement | 13.88 | – |
| Cement with fly ash | 16.17 | 16% |
| Cement with bentonite | 19.31 | 39% |

low saturated adsorption capacity for TN. Overall, the results showed that the structure of the pervious concrete pavement can be optimized for improved function. Future research should focus on the use of additives in the base layer and modification of additives to increase the contact area with runoff pollution. Additionally, the quantities of additives should be optimized to provide the theoretical basis for engineering applications.

1. Nnadi, E. O., Newman, A. P., Coupe, S. J. and Mbanaso. F. U., Stormwater harvesting for irrigation purposes: an investigation of chemical quality of water recycled in pervious pavement system. *J. Environ. Manage.*, 2015, **147**, 246–256.
2. Fassman, E. A. and Blackbourn, S. D., Road runoff water-quality mitigation by permeable modular concrete pavers. *J. Irrig. Drain. Eng.*, 2011, **137**, 720–729.
3. Lucke, T. and Beecham, S. E., Filed investigation of clogging in a permeable pavement system. *Build. Res. Inf.*, 2011, **39**, 603–615.

4. Rukai, L., Xiaoming, W., Huoming, W. and Gang, Z., Research on adhesive dosage of porous polyurethane gravel pavement. *Highway Eng.*, 2015, **40**, 105–108.
5. Qiushi, L. and Dongpo, H., Comparative study of porous concretes using naturaland recycled aggregates. *J. Beijing Univ. Technol.*, 2015, **41**, 89–94.
6. Zhang, P., Zhao, Y. N., Li, Q., Wang, P. and Zhang, T. H., Flexural toughness of steel fiber reinforced high performance concrete containing nano-$SiO_2$ and fly ash. *Curr. Sci.*, 2014, **106**, 980–987.
7. Blissett, R. S. and Rowson, N. A., A review of the multi-component utilization of coal fly ash. *Fuel*, 2012, **97**, 1–23.
8. Berez, A., Schäfer, G., Ayari, F. and Trabelsi-Ayadi, M., Adsorptive removal of azo dyes from aqueous solutions by natural bentonite under static and dynamic flow conditions. *Int. J. Environ. Sci. Technol.*, 2016, **13**(7), 1625–1640.
9. Gao, Y., Zhu, B., Yu, G., Chen, W., He, N., Wang, T. and Miao, C., Coupled effects of biogeochemical and hydrological processes on C, N, and P export during extreme rainfall events in a purple soil watershed in southwestern China. *J. Hydrol.*, 2014, **511**, 692–702.
10. Li, L. and Davis, A. P., Urban stormwater runoff nitrogen composition and fate in bioretention systems. *Environ. Sci. Technol.*, 2014, **48**, 3403–3412.
11. Zinger, Y., Blecken, G. T., Fletcher, T. D., Viklander, M. and Deletić, A., Optimising nitrogen removal in existing stormwater-biofilters: benefits and tradeoffs of a retrofitted saturated zone. *Ecol. Eng.*, 2013, **51**, 75–82.
12. Liu, J. and Davis, A. P., Phosphorus speciation and treatment using enhanced phosphorus removal bioretention. *Environ. Sci. Technol.*, 2014, **48**, 607–620.
13. Wang, B., Li, T., Meng, Y., Ren, Z. and Cao, B., Distribution from of nutrients in roof runoff. *Environ. Sci.*, 2008, **29**, 3035–3042.
14. Jeppu, G. P. and Clement, T. P., A modified Langmuir-Freundlich isotherm model for simulating pH-dependent adsorption effects. *J. Contam. Hydrol.*, 2012, **129**.
15. Phetphaisit, C. W., Yuanyang, S. and Chaiyasith, W. C., Polyacrylamido-2-methyl-1-propane sulfonic acid-grafted-natural rubber as bio-adsorbent for heavy metal removal from aqueous standard solution and industrial wastewater. *J. Hazard. Mater.*, 2015, **301**, 163–171.
16. Park, C. M., Chu, K. H., Heo, J., Her, N., Jang, M., Son, A. and Yoon, Y., Environmental behavior of engineered nanomaterials in porous media: a review. *J. Hazard. Mater.*, 2016, **309**, 133–150.
17. Mahmoodian, H. *et al.*, Enhanced removal of methyl orange from aqueous solutions by poly HEMA–chitosan-MWCNT nanocomposite. *J. Mol. Liq.*, 2015, **202**, 189–198.
18. Latour, R. A., The langmuir isotherm: A commonly applied but misleading approach for the analysis of protein adsorption behavior. *J. Biomed. Mater. Res. A*, 2015, **103**, 949–958.
19. Ghosal, P. S. and Gupta, A. K., Determination of thermodynamic parameters from Langmuir isotherm constant-revisited. *J. Mol. Liq.*, 2016, **225**, 137–146.
20. Xia, L. X., Shen, Z., Vargas, T., Sun, W. J. and Ruan, R. M., Attachment of Acidithiobacillus ferrooxidans onto different solid substrates and fitting through Langmuir and Freundlich equations. *Biotechnol. Lett.*, 2013, **35**, 2129–2136.
21. Nakkeeran, E. *et al.*, Hexavalent chromium removal from aqueous solutions by a novel powder prepared from Colocasia esculenta leaves. *Int. J. Phytoremediation*, 2016, **42**, 812–821.
22. Saranya, N., Nakkeeran, E., Shrihari, S. and Selvaraju, N., Equilibrium and kinetic studies of hexavalent chromium removal using a novel biosorbent-Ruellia patula Jacq. *Arab. J. Sci. Eng.*, 2017, **18**, 1545–1557.
23. Çınar, S. *et al.*, An efficient removal of RB5 from aqueous solution by adsorption onto nano-ZnO/Chitosan composite beads. *Int. J. Biol. Macromol.*, 2017, **96**, 459–465.
24. Guangxing, Z. *et al.*, Adsorption and desorption of ammonia-nitrogen wastewater by modified bentonite. *Chin. J. Environ. Eng.*, 2017, **11**, 1494–1500.

ACKNOWLEDGEMENTS. We acknowledge the funding support from the Major Science and Technology Program for Water Pollution Control and Treatment of China (2010ZX07302-002) and the technology support obtained from the Key Laboratory of Urban Stormwater System and Water Environment (Beijing University of Civil Engineering and Architecture), Ministry of Education.

Received 11 January 2017; accepted 8 July 2017

doi: 10.18520/cs/v114/i02/378-384

# Climate change-induced coral bleaching in Malvan Marine Sanctuary, Maharashtra, India

**K. Diraviya Raj[1,*], G. Mathews[1], M. Selva Bharath[1], Rohit D. Sawant[2], Vishal Bhave[3], Deepak Apte[3], N. Vasudevan[2] and J. K. Patterson Edward[1]**

[1]Suganthi Devadason Marine Research Institute, 44-Beach Road, Tuticorin 628 001, India
[2]UNDP Sindhudurg Project and Mancrove Cell, Mumbai 400 051, India
[3]Bombay Natural History Society, Mumbai 400 001, India

**Malvan Marine Sanctuary (MMS), Maharashtra, India is rich in coral reefs and the associated resources, which provide livelihood for the people involved in fishing and tourism. The elevated sea-surface temperature triggered by climate change had caused the coral reefs around the world to undergo severe bleaching during 2014–2016. Scientists have declared this as the third global coral bleaching event. Two underwater surveys during December 2015 and May 2016 were conducted in MMS to assess the intensity and trend of coral bleaching. A high prevalence of coral bleaching, i.e. 70.93% (SD = 4.53) was recorded inside MMS during December 2015, with a mortality of about 8.38% (SD = 0.91). After a lapse of six months, corals were found to recover. This is borne out by the reduction in the bleaching prevalence to 6.77 ± 0.12% during May 2016. Climate change being a global issue, reduction in the local stressors such as fishing and tourism is highly recommended in order to allow the corals to recover and enable sustainable utilization of coral reef resources around MMS.**

*For correspondence. (e-mail: diraviyam_raj@yahoo.co.in)